Flexible Multi-Colored Electrochromic and Volatile Polymer Memory Devices Derived from Starburst Triarylamine-Based Electroactive Polyimide

*Hung-Ju Yen, Chih-Jung Chen, and Guey-Sheng Liou**

Flexible multi-colored electrochromic and volatile memory devices are fabricated from a solution-processable electroactive aromatic polyimide with starburst triarylamine unit. The polyimide prepared by the chemical imidization was highly soluble in many organic solvents and showed useful levels of thermal stability associated with high glass-transition temperatures. The polyimide with strong electron-donating capability possesses static random access memory behavior and longer retention time than other 6FDA-based polyimides. The differences of the highest-occupied and lowest unoccupied molecular orbital levels among these polyimides with different electron-donating moieties are investigated and the effect on the memory behavior is demonstrated. The polymer film shows reversible electrochemical oxidation and electrochromism with high contrast ratio both in the visible range and near-infrared region, which also exhibits high coloration efficiency, low switching time, and the outstanding stability for long-term electrochromic operation. The highly stable electrochromism and interesting volatile memory performance are promising properties for the practical flexible electronics applications in the future.

1. Introduction

Nowadays, the application of polymeric material in optoelectronic devices has attracted tremendous attention, for example in light-emitting diodes,[1] solar cells,[2] electrochromic (EC) devices,[3] and memory devices.[4] Donor–acceptor containing polymers include both electron donor and acceptor moieties within a repeating unit, which can be switched between two conductive states via electrical field are widely researched for resistive switching memory applications recently.[4] By virtue of their flexible device structure, low cost, long range processability, three-dimensional stacking capability for high density data storage, and the possibility of modulating,[5] electrically bistable resistive switching devices based on polymeric materials have significant advantages over inorganic silicon- and metal-oxide-based memory materials.[6]

Among the different polymeric systems that have been researched, the charge transfer (CT) effect is one of the most interesting mechanisms for inducing resistor-type polymer memory (RRAM) behavior by introducing the electron donor and the electron acceptor moieties into the repeat unit of the polymer. Under an applied electric field, charge transfer will occur resulting in a transfer of electronic charge from the donor to the acceptor moiety, and the resulting structure can be defined as CT complex (CTC).[7] The stability of the CTC is regarded as one of the crucial factors for its memory behavior. Therefore, we have demonstrated the importance of structural effects tuned by incorporating different dianhydrides (electron accepter) into triphenylamine (TPA)-based polyimide backbone on the relaxation time of the polymeric memory.[8] These polyimides with different electron-withdrawing intensity revealed intriguing properties from volatile dynamic random access memory (DRAM) for **6FPI**, static random access memory (SRAM) for **PMPI** to non-volatile write-once-read-many-times (WORM) for both **DSPI** and **NPPI**, respectively. Moreover, studies based on polyimides derived from diamines having different electron-donating capability with the same electron-withdrawing dianhydride were also reported by Kang and Ree; the devices fabricated by TPA-based polyimide **TPA-6FPI**[4a] and phenylamine-substituted **2TPA-6FPI**[4b] exhibited DRAM and WORM behavior, respectively. However, the systematic research about the effect of an electron-donor moiety within a donor–accepter polyimide backbone system on the memory properties—especially for polymer memory exhibiting SRAM behavior requiring more stable CTCs resulting from the stronger electron donor—has not yet been reported.

High-performance polymers (e.g., polyimide and polyamide[4f]) containing electron donating triarylamines moiety are favorable functional materials not only for memory devices due to their excellent thermal dimensional stability, chemical resistance, mechanical strength, and high ON/OFF current ratio,[9] but also for EC applications.[10] Since 2005, our group has reported several TPA-containing anodic EC polymers

Dr. H.-J. Yen, C.-J. Chen, Prof. G.-S. Liou
Functional Polymeric Materials Laboratory
Institute of Polymer Science and Engineering
National Taiwan University
1 Roosevelt Road, 4th Sec., Taipei 10617, Taiwan
E-mail: gsliou@ntu.edu.tw

DOI: 10.1002/adfm.201300569

with interesting color transitions,[10] which showed excellent EC reversibility in the visible region and NIR range. However, most of the EC polymers developed so far only revealed less than two stage EC behavior as EC devices (ECD) or were utilized for preliminary solution spectroelectrochemical investigation due to the difficulty and complexity in preparing triarylamine-containing structures with more electroactive sites. Therefore, our strategy in this work is to synthesize the starburst triarylamine-based polyimide for both polymeric volatile memory and multi-colored EC devices. By incorporating the electron-donating starburst triarylamine moiety with methoxyl-group at the *para*-position of phenyl groups, the coupling reactions of the prepared polyimide could be greatly prevented by affording stable cationic radicals with a lower oxidation potential (higher HOMO energy level).[11] The resulting electroactive polymers with high molecular weights and excellent thermal stability should be obtained readily by using conventional polycondensation. Because of the incorporation of packing-disruptive starburst triarylamine units into the polymer backbone, these novel polymers should also have excellent solubility in various polar organic solvents, thus transparent and flexible polymer thin films could be prepared easily by solution casting and spin-coating techniques. This is beneficial for their fabrication of large-area, thin-film optoelectronic devices.

In this contribution, we synthesized the aromatic polyimide containing starburst triarylamine units from the diamine monomer, *N*,*N*-bis[4-(4-methoxyphenyl-4′-aminophenylamino) phenyl]-*N*′,*N*′-di(4-methoxyphenyl)-*p*-phenylenediamine (**1**).[3b] The incorporation of electron-donating starburst triarylamine units is expected to lower the oxidation potential associated with increasing electrochemical stability and multi-stage EC characteristic. Moreover, we anticipate that the novel polyimide also could reveal more stable CTC resulting in longer retention time of memory device. Thus, the flexible multi-colored EC and polymeric memory devices were fabricated and investigated systematically in this study (**Figure 1**).

2. Results and Discussion

2.1. Synthesis and Basic Characterization of Polyimide

The new starburst polyimide **9Ph-6FDA** was prepared by the reaction of diamine **1** with commercially available 4,4′-(hexafluoroisopropylidene)diphthalic anhydride (**6FDA)** in *N*-methyl-2-pyrrolidinone (NMP) at room temperature to form the precursor poly(amic acid), followed by chemical imidization (**Scheme 1**). In the first step, the reaction mixture became very viscous as poly(amic acid) was formed, indicating the formation of high molecular weight polymer. The poly(amic acid) precursor could be chemically dehydrated to the polyimide by treatment with acetic anhydride and pyridine. The polymerization reaction proceeded homogenously and gave high molecular weight, which could afford transparent and tough films via solution casting. Polyimide **9Ph-6FDA** had an inherent viscosity of 43.0 L/mg with weight-average molecular weight (M_w) and polydispersity (PDI) of 161 800 Da and 1.94, respectively, relative to polystyrene standards (Supporting Information Table S1). The structure of polyimide **9Ph-6FDA** was confirmed by NMR and IR spectroscopy. The ^{1}H NMR spectrum was illustrated in Supporting Information Figure S1 and agreed well with the proposed molecular structure. As shown in Supporting Information

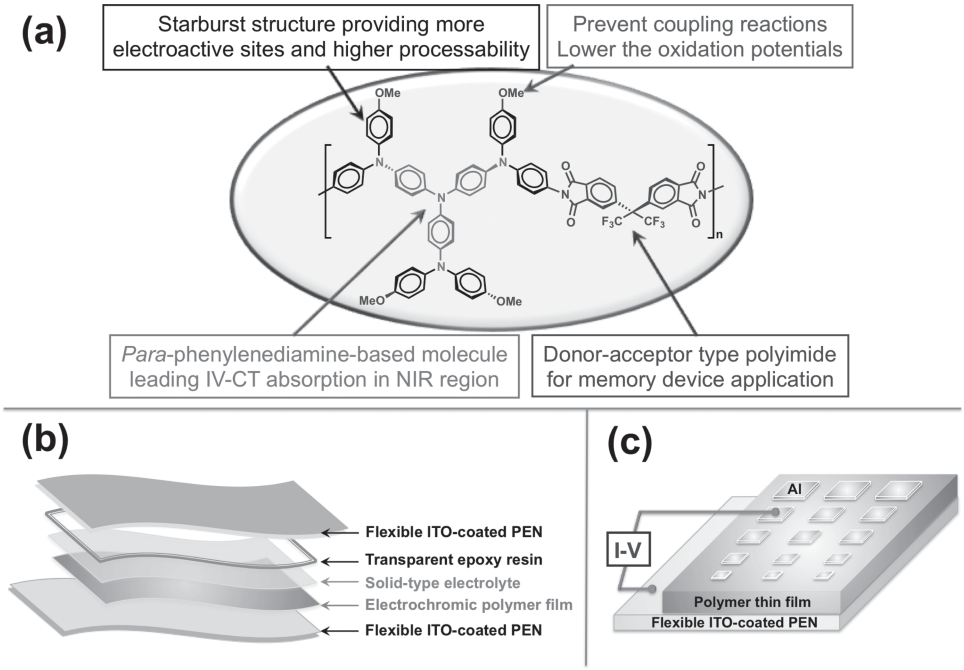

Figure 1. a) Design strategy of starburst triarylamine-based polyimide **9Ph-6FDA**, b) schematic diagram of flexible EC device based on single-layer EC polyimide, and c) configuration of the flexible memory device consisting of the polyimide thin film sandwiched between an ITO bottom electrode and an Al top electrode.

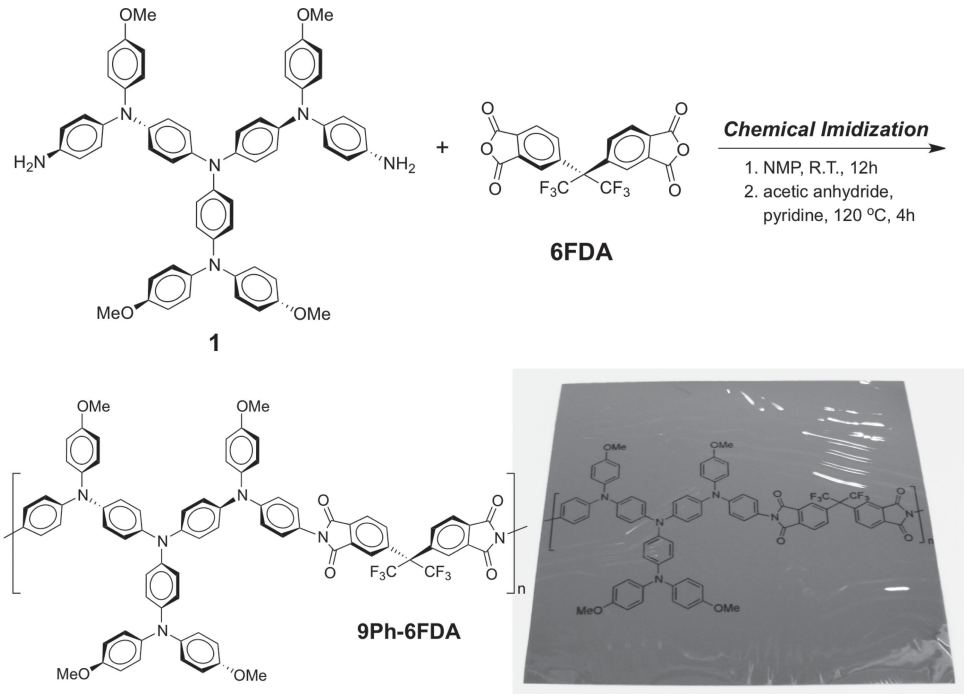

Scheme 1. Synthesis of aromatic polyimide **9Ph-6FDA**. The photograph shows appearance of the flexible film (thickness: ≈20 μm).

Figure S2, a typical IR spectrum exhibited characteristic imide absorption bands at around 1783 (asymmetrical C = O), 1721 (symmetrical C = O), 1379 (C–N), and 720 cm^{-1} (imide ring deformation).

The solubility property of polyimide **9Ph-6FDA** was investigated at 5% w/v concentration and the results are also listed in Supporting Information Table S2. Polyimide **9Ph-6FDA** was highly soluble not only in polar aprotic organic solvents such as NMP, *N,N*-dimethylacetamide (DMAc), *N,N*-dimethylformamide (DMF), dimethyl sulfoxide (DMSO) but also in less polar solvents such as tetrahydrofuran (THF) and $CHCl_3$, which could be attributed to the incorporation of bulky and three-dimensional starburst triarylamine moiety along the polymer backbone, resulting in high steric hindrance for close packing. In addition, the excellent solubility makes the polymer as potential candidate for practical applications by spin-coating or inkjet-printing processes to afford high performance thin film for optoelectronic devices. Thus, the polyimide **9Ph-6FDA** could be solution-cast into a flexible, transparent, and tough film; the appearance of the film is shown in Scheme 1.

The thermal properties of polyimide **9Ph-6FDA** were examined by TGA and TMA, and the thermal behavior data are summarized in Supporting Information Table S3. TGA and TMA curves of polyimide **9Ph-6FDA** are shown in Supporting Information Figure S3. The prepared polyimide exhibited good thermal stability with insignificant weight loss up to 350 °C even with the introduction of methoxy groups, and the carbonized residue (char yield) of these polymers in a nitrogen atmosphere was more than 64% at 800 °C. The glass-transition temperature (T_g) could be easily measured at 266 °C in the TMA thermogram (as shown in Supporting Information Figure S3).

2.2. Absorption and Electrochemistry

The UV-vis absorption spectrum of polyimide **9Ph-6FDA** is provided in Supporting Information Figure S4 and the onset wavelength of optical absorption was utilized to obtain the optical energy band gap (E_g) of the polyimide. The electrochemical properties of polyimide **9Ph-6FDA** were investigated by cyclic voltammetry (CV), and was conducted by cast film on an indium-tin oxide (ITO)-coated glass slide as working electrode in anhydrous acetonitrile (CH_3CN), using 0.1 M of tetrabutylammonium perchlorate (TBAP) as a supporting electrolyte in a nitrogen atmosphere. Typical CV diagrams for polyimide **9Ph-6FDA** are shown in **Figure 2**, revealing four reversible oxidation redox couples. During the electrochemical oxidation of the polyimide thin film, the color of polymer film changed from colorless to yellow, purple, blue, and then to black. Because of the high electrochemical stability and good adhesion between the polyimide thin film and ITO substrate, polyimide **9Ph-6FDA** exhibited highly reversible CV behavior by continuous 10 000 cyclic scans in the second oxidation stage. The redox potentials of the polyimide as well as their respective highest occupied molecular orbital (HOMO) and lowest unoccupied molecular orbital (LUMO) (vs vacuum) are calculated and summarized in **Table 1**. The HOMO level or called ionization potentials (versus vacuum) of polyimide **9Ph-6FDA** could be estimated from the onset of their oxidation in CV experiments as 4.78 eV (on the basis that ferrocene/ferrocenium is 4.8 eV below the vacuum level with E_{onset} = 0.36 V).

2.3. Memory Device Characteristics

The memory behavior of **9Ph-6FDA** was investigated by the current–voltage (*I–V*) characteristics of an ITO-coated

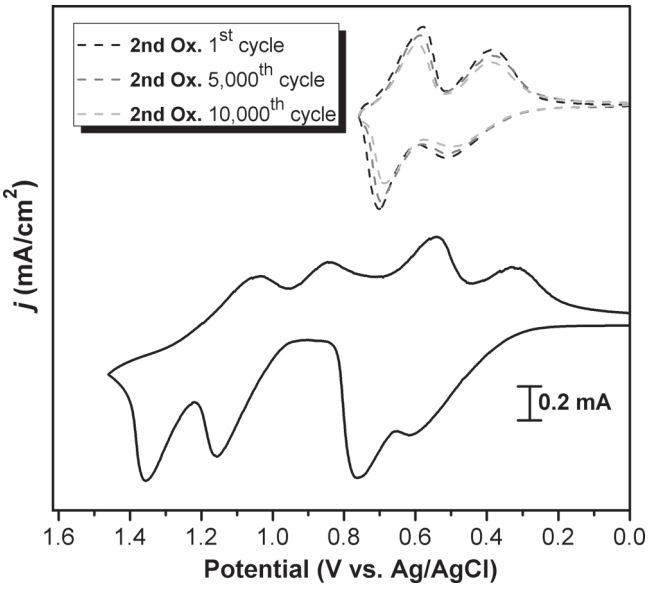

Figure 2. Cyclic voltammograms of polyimide **9Ph-6FDA** film on an ITO-coated glass substrate with continuous cyclic scans in 0.1 M TBAP/CH_3CN at a scan rate of 50 mV/s.

PEN/9Ph-6FDA/Al sandwich device as shown in Figure 1c. Within the flexible device, polymer film was used as an active layer between Al and ITO as the top and bottom electrodes. To exclude the effect of the polymer film thickness on memory properties, a standard thickness (50 nm) was used without specific mention.

Figure 3a reveals the *I–V* result of **9Ph-6FDA** memory device. A sharp increasing of the current could be observed at –3.7 V during the negative sweep, indicating that the device undergoes an electrical transition from the OFF state to the ON state. The device remained in the ON state during the subsequent negative (the third sweep) and positive scans (the fourth sweep). Interestingly, the device of **9Ph-6FDA** still maintained in the ON state after turning off the power for a longer period of time than in the cases of **3Ph-6FDA**[4a] and **5Ph-6FDA**.[8] The fifth sweep was conducted after turning off the power for about 3 min, and found that the ON state had relaxed to the steady OFF state without an erasing process, but the device could be switched to the ON state again at the threshold voltage of –3.6 V, and the sixth sweep was conducted to make sure that the device could be remained in the ON state again. The longer retention time at the ON state before volatile as well as the randomly accessible ON and OFF states are similar to the data remanence behavior of SRAM. To confirm the feasibility of the switching performance of flexible device, the device was further characterized by physically fixing with a vernier caliper from flat to bent conditions (Figure 3b). The memory device was tested under severe bending at various curvature radii of 11, 9, 7, and 5 mm, respectively, and the flexible device did not crack or deform upon bending. The reliable and reproducible switching memory behavior of polymer film in the device (Figure 3c) also could be obtained under mechanical bending stress. To gain more insight into the memory behavior of the polymeric devices, the molecular orbital and electric density contours of the basic units were estimated in detail by molecular simulation.

Table 1. Redox potentials and energy levels of **9Ph-6FDA**.

Polymer	Thin films [nm]		Oxidation potential [V][a]					E_g [eV][b]	HOMO [eV][c]	LUMO [eV]
	λ_{max}	λ_{onset}	E_{onset}	$E_{1/2(ox1)}$	$E_{1/2(ox2)}$	$E_{1/2(ox3)}$	$E_{1/2(ox4)}$			
9Ph-6FDA	345	564	0.34	0.46	0.65	1.02	1.19	2.20	4.78	2.58

[a]From cyclic votammograms vs. Ag/AgCl in CH_3CN. $E_{1/2}$: average potential of the redox couple peaks; [b]The data were calculated from polymer films by the equation: $E_g = 1240/\lambda_{onset}$ (energy gap between HOMO and LUMO); [c]The HOMO energy levels were calculated from cyclic voltammetry and were referenced to ferrocene (4.8 eV; onset = 0.36 V).

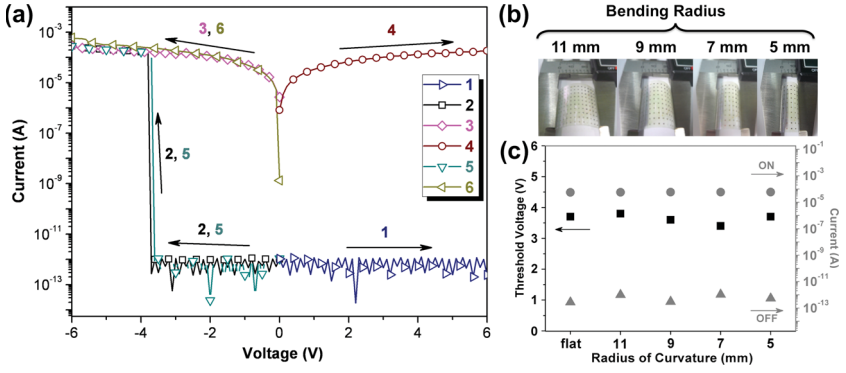

Figure 3. a) Current-voltage (*I–V*) characteristics, b) appearance in various bent states, and c) variation of current and threshold voltage with different bending radii of the ITO/**9Ph-6FDA** (50 ± 3 nm)/Al flexible memory device.

2.4. Switching Mechanism

The molecular simulation on the basic units of **3Ph-6FDA**, **5Ph-6FDA**, and **9Ph-6FDA** was carried out by DFT/B3LYP/6-31G(d) with the Gaussian 09 program. The charge density isosurfaces of the basic unit, the most energetically favorable geometry, HOMO and LUMO energy levels are summarized in **Figure 4**. The LUMO energy levels calculated by molecular simulation could be taken as evidence to indicate the electron-withdrawing ability of **6FDA**. For these TPA based polyimides systems, the HOMO energy levels were located mainly at the electron-donating TPA derivative moieties, while the LUMO energy levels were located at the electron-withdrawing phthalimide units.

As shown in Figure 4, with increasing the electron donating ability of TPA derivatives in polyimides (higher HOMO energy levels) from **3Ph-6FPI** to **9Ph-6FPI**, a more stable charge transfer complex could be obtained. Thus, polyimides with 6FDA possess DRAM property for **3Ph-6FDA** and **5Ph-6FDA** while SRAM behavior for **9Ph-6FDA**. These results revealed that the increase

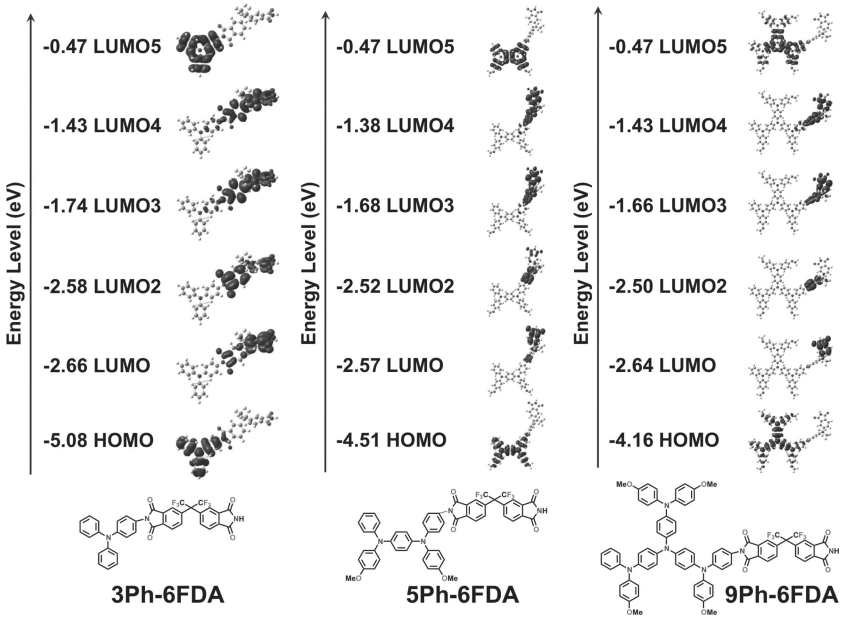

Figure 4. Calculated molecular orbitals and corresponding energy levels of the basic units for **6FDA**-based polyimides.

of electron-donating ability from **3Ph-6FDA** to **9Ph-6FDA** would contribute to the enhancement of retention time of the memory device. Thus, with the design of chemical structure, tunable memory properties with different retention time could be obtained.

2.5. Spectroelectrochemical and Electrochromic Properties

Spectroelectrochemical experiments were used to evaluate the optical properties of the EC films. For the investigation, polyimide film was prepared in the same manner as described above, and a home-made electrochemical cell was built from a commercial ultraviolet (UV)-visible cuvette. The cell was placed in the optical path of the sample light beam in a UV-vis-NIR spectrophotometer, which allowed us to acquire electronic absorption spectra under potential control. UV-vis-NIR absorbance curves correlated to electrode potentials of polyimide **9Ph-6FDA** are presented in **Figure 5**, which were reversible and associated with strong color changes.

In the neutral form (0 V), the film exhibited strong absorption at around 345 nm, characteristic for triarylamine, but it was almost transparent in the visible region. Upon oxidation (increasing applied voltage from 0 to 0.60 V), the intensity of the absorption peak at 345 nm gradually decreased while a new peak at 441 nm and a broad IV-CT band centered around 1100 nm in the NIR region gradually increased in intensity. The first oxidation reversibility was 99% based on the absorbance at 345 nm.[12] We attribute the spectral change in visible light range to the formation of a stable monocation radical **9Ph-6FDA**$^{1+}$ in the TPA center of starburst triarylamine moiety. Furthermore, the broad absorption in NIR region was the characteristic result due to IV-CT excitation between states in which the positive charge is centered at different nitrogen atoms, which is consistent with the phenomenon reported by Robin and Day.[13] Meanwhile, the color of the film changed from colorless (L^*, 96; a^*, –2; b^*, 3) to yellow (L^*, 85; a^*, –11; b^*, 53). As the more anodic potential to 0.90 V corresponding to **9Ph-6FDA**$^{2+}$, the absorption bands (345 and 441 nm) decreased gradually with new broad bands centered at around 540 and 1050 nm, and the film became purple in color (L^*, 69; a^*, 2; b^*, –8) during the second oxidation with a reversibility of 95%. By further applying positive potential value up to 1.20 V corresponding to **9Ph-6FDA**$^{3+}$, the characteristic absorbance at 600 and 795 nm appeared, and the strong IV-CT band at 1060 nm in the NIR region still could be observed with a reversibility of 75%. As shown in Figure 5, the polymer film turned to a deep blue color (L^*, 50; a^*, 5; b^*, –26). When the applied potential was added to 1.50 V, the absorption bands revealed a broad visible absorption

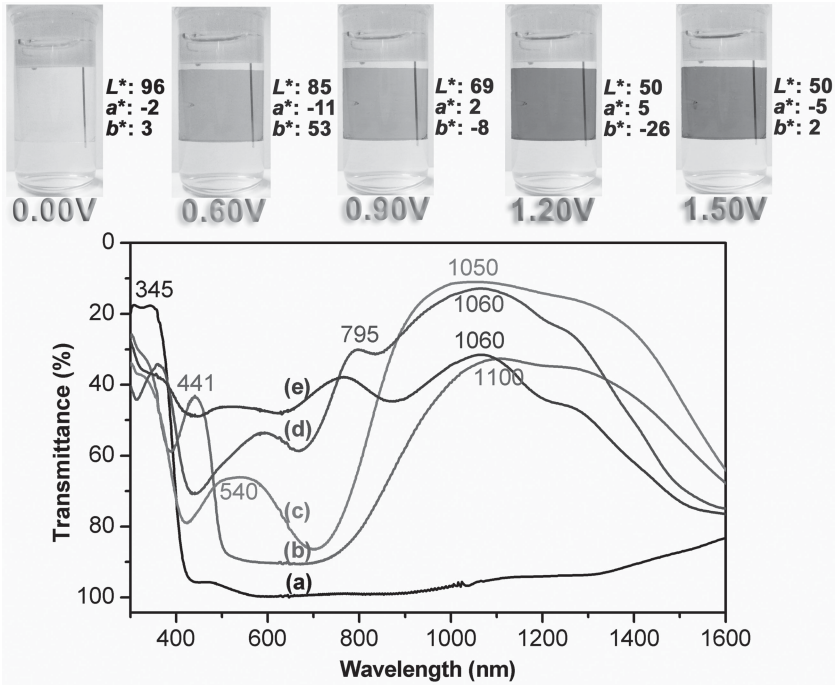

Figure 5. EC behavior at applied potentials of a) 0.00, b) 0.60, c) 0.90, d) 1.20, e) 1.50 V (vs. Ag/AgCl) of polyimide **9Ph-6FDA** thin film (130 ± 10 nm in thickness) on the ITO-coated glass substrate in 0.1 M TBAP/CH_3CN.

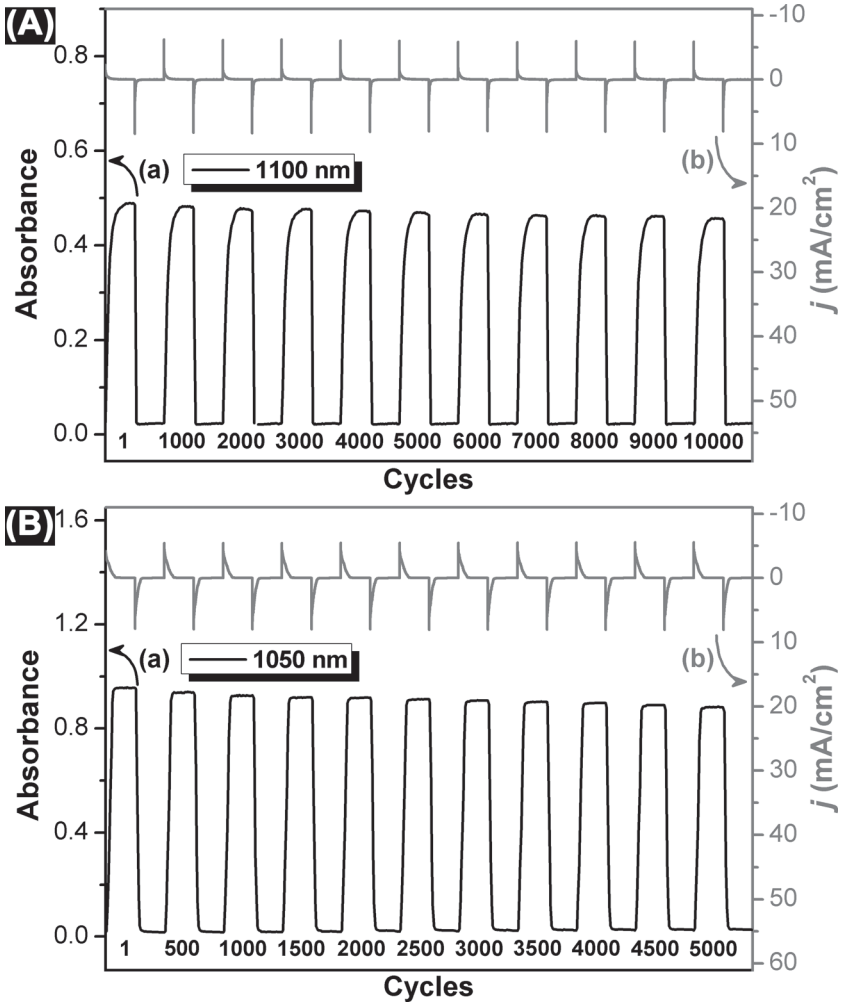

Figure 6. EC switching between A) 0 and 0.60 V and B) 0 and 0.90 V (vs. Ag/AgCl) of polyimide **9Ph-6FDA** thin film (130 ± 10 nm in thickness) on the ITO-coated glass substrate (coated area: 1.2 cm × 0.5 cm) in 0.1 M TBAP/CH_3CN with a cycle time of 30 s. a) Absorbance change and b) current consumption monitored at the given wavelength.

from 400 to 800 nm with a good combination of the NIR absorption, but only 50% absorbance remained implying that the oxidation product (tetracation) was not stable. At the final stage, the absorption band can be attributed to the further oxidation of the **9Ph-6FDA**$^{3+}$ species to **9Ph-6FDA**$^{4+}$ in the starburst triarylamine segments; at this stage the polymer film turned black in color (L^*, 50; a^*, -5; b^*, 2). The colorimetric result is consistent with the absorption spectra of **9Ph-6FDA** thin film as a small amount of blue and green light is transmitted.

The film coloration is distributed homogeneously across the polymer film and reveal excellent stability for more than 1000 redox cycles. The polyimide **9Ph-6FDA** shows good contrast both in the visible and NIR regions with an extremely high optical transmittance change ($\Delta\%T$) of 85% at 1050 nm for purple coloring at the second oxidation stage, and 69% at 795 nm for blue coloring at the third oxidation stage, respectively. Because of the apparent high EC contrast, optical switching studies were investigated more deeply to manifest the outstanding EC characteristics of the novel anodically EC material.

2.6. Electrochromic Switching Studies

For EC switching studies, polymer films were cast on ITO-coated glass slides in the same manner as described above, and chronoamperometric and absorbance measurements were performed. While the films were switched, the absorbance at given wavelength was monitored as a function of time with UV-vis-NIR spectroscopy. Switching data for the representative cast film of polyimide **9Ph-6FDA** were shown in Supporting Information Figure S5 and **Figure 6**. The switching time was calculated at 90% of the full switch because it is difficult to perceive any further color change with the naked eye beyond this point. As depicted in Supporting Information Figure S5a, when the potential was switched between 0 and 0.60 V, polyimide **9Ph-6FDA** thin film had a switching time of 3.60 s for the coloring process and 0.90 s for bleaching. When the switching potential was set between 0 and 0.90 V, thin film **9Ph-6FDA** required 3.15 s for coloration and 1.90 s for bleaching (Supporting Information Figure S5b). The polyimide switched rapidly between the highly transmissive neutral state and the colored oxidized states. The amount of injected/ejected charge (Q) were calculated by integration of the current density and time obtained from Supporting Information Figure S5c as 2.067 mC/cm^2 and 2.050 mC/cm^2 for oxidation and reduction processes at the first oxidation stage, respectively. The ratio of the charge density was 99.2%, indicating that charge injected/ejected was highly reversible during the electrochemical reactions. As shown in Figure 6, the EC stability of the polyimide **9Ph-6FDA** film was determined by measuring the optical change as a function of the number of switching cycles. The EC CE ($\eta = \delta OD/Q$) and injected charge (electroactivity) after various switching steps were monitored and summarized in **Table 2** and **Table 3**. The EC film of **9Ph-6FDA** was found to exhibit high CE up to 223 cm^2/C at 1100 nm, and to retain more than 98% of the electroactivity after switching 10 000 times between 0 and 0.60 V (Figure 6a). As the applied switching potential increased to 0.90 V, a higher CE (272 cm^2/C at 1050 nm) could be obtained and showed only 1.7% decay of its electroactivity after 5000 cycles (Figure 6b).

Furthermore, we also fabricated single layer flexible EC cells based on polyimide **9Ph-6FDA** for long-term stability and bending investigations (**Figure 7**). The polymer film is colorless in neutral form. When the voltage was increased consecutively (to a maximum of 3.0 V), the color changed to yellow, purple, blue, and then to black due to electro-oxidation, the same as that was already observed in the spectroelectrochemical experiments. The polymer film turned back to its original colorless form when the potential was subsequently set back at 0 V.

Table 2. Optical and electrochemical data collected for coloration efficiency measurements of **9Ph-6FDA**.

Cycling Times[a)]	δOD_{1100}[b)]	Q [mC/cm^2][c)]	η [cm^2/C][d)]	Decay [%][e)]
1	0.461	2.067	223	0
1000	0.454	2.064	220	1.36
2000	0.449	2.058	218	2.16
3000	0.453	2.053	221	1.05
4000	0.448	2.049	219	1.95
5000	0.443	2.044	217	2.81
6000	0.441	2.039	216	3.01
7000	0.438	2.037	215	3.58
8000	0.437	2.036	215	3.75
9000	0.437	2.034	215	3.66
10 000	0.432	2.030	213	4.57

[a)]Switching between 0.00 and 0.60 (V vs. Ag/AgCl); [b)]Optical density change at 1100 nm; [c)]Ejected charge, determined from the in situ experiments; [d)]Coloration efficiency is derived from the equation: $\eta = \delta OD_{1100}/Q$; [e)]Decay of coloration efficiency after cyclic scans.

During the long-term stability measurement by keeping 10 h for each coloring stage at applied potentials of 0.60 and 0.90 V, respectively, extremely high EC stability was observed, which reinforces and affords positive proof of the NIR electroactive aromatic polyimide with potential for commercial applications.

The flexible EC device was also characterized by physically fixing it in the same manner as described above (Supporting Information Figure S6a). The transmittance response of the flexible memory device with various bending radius were analyzed in detail and shown in Supporting Information Figure S6b, which suggests good flexibility and mechanical endurance. The severe bending of the EC device at various curvature radii of 20, 15, 10, and 5 mm does not degrade the device behavior, revealing that the flexible EC device is reliable even when the substrate is severely bent. Considering the retained contrast ratio and electroactive stability during EC operation, the novel polyimide shows the highest EC stability to the best of our knowledge compared with other EC polymers.[3,14] We believe that optimization could further improve the device performance to fully explore the potential of the EC polyimide.

Table 3. Optical and electrochemical data collected for coloration efficiency measurements of **9Ph-6FDA**.

Cycling Times[a)]	δOD_{1050}[b)]	Q [mC/cm^2][c)]	η [cm^2/C][d)]	Decay [%][e)]
1	0.939	3.452	272	0
500	0.921	3.448	267	1.80
1000	0.911	3.445	264	2.78
1500	0.903	3.439	263	3.46
2000	0.902	3.435	263	3.46
2500	0.895	3.428	261	4.01
3000	0.890	3.420	260	4.33
3500	0.885	3.414	259	4.70
4000	0.880	3.408	258	5.07
4500	0.873	3.401	257	5.63
5000	0.865	3.393	255	6.27

[a)]Switching between 0.00 and 0.90 (V vs. Ag/AgCl); [b)]Optical density change at 1050 nm; [c)]Ejected charge, determined from the in situ experiments; [d)]Coloration efficiency is derived from the equation: $\eta = \delta OD_{1050}/Q$; [e)]Decay of coloration efficiency after cyclic scans.

3. Conclusions

A novel aromatic polyimide with starburst triarylamine units was readily prepared from the diamine monomer, *N*,*N*-bis[4-(4-methoxyphenyl-4′-aminophenylamino)phenyl]-*N*′,*N*′-di(4-methoxyphenyl)-*p*-phenylenediamine, with aromatic dianhydride **6FDA** via chemical polyimidization. Introduction of highly electron-donating starburst triarylamine group to the polymer main chain not only stabilizes its radical cations but also leads to good solubility and film-forming properties of the polyimide. In addition to high T_g and good thermal stability, the obtained polymer also revealed valuable optoelectronic properties such as memory and EC behavior. The polyimide **9Ph-6FDA** with strong electron-donating capability possesses SRAM memory behavior and longer retention time. The EC polyimide film shows reversible electrochemistry with high contrast ratio and the outstanding stability for long-term EC operation. Thus, these characteristics suggest that the novel starburst triarylamine-containing aromatic polyimide has great potential for the practical flexible electronics applications in the future.

4. Experimental Section

Materials: *N*,*N*-Bis[4-(4-methoxyphenyl-4′-aminophenylamino)phenyl]-*N*′,*N*′-di(4-methoxyphenyl)-*p*-phenylenediamine (**1**)[3b] was synthesized according to a previously reported procedure. Commercially available 4,4′-(hexafluoroisopropylidene)diphthalic anhydride (**6FDA**) (Chriskev) was purified by vacuum sublimation. Tetrabutylammonium perchlorate (TBAP) (Acros) was recrystallized twice by ethyl acetate in a nitrogen atmosphere and then dried in vacuo prior to use. All other reagents were used as received from commercial sources.

Polymer Synthesis: To a solution of 0.47 g (0.53 mmol) of diamine **1** in 5.0 mL of NMP, 0.23 g (0.53 mmol) of dianhydride **6FDA** was added in one portion. The mixture was stirred at room temperature overnight (ca. 12 h) to afford a viscous poly(amic acid) solution. The poly(amic acid) was subsequently converted to polyimide **9Ph-6FDA** via a chemical imidization process by addition of pyridine 1 mL and acetic anhydride 2 mL, then the mixture was heated at 120 °C for 4 h to effect complete imidization. The obtained polymer solution was poured slowly into 300 mL of stirred methanol giving rise to stringy and fiber-like precipitate that was collected by filtration, washed thoroughly with and methanol, and dried under vacuum at 100 °C. Reprecipitation of the polymer by DMAc/methanol was carried out twice for further purification. The inherent viscosity and weight-average molecular weight (M_w) of the obtained polyimide was 43.0 L/mg (measured at a concentration of 5.0 g/L in DMAc at 30 °C) and 161 800 Da, respectively. The FT-IR spectrum exhibited characteristic imide absorption bands at 1783 (asymmetrical C = O), 1721 (symmetrical C = O), 1379 (C–N), and 720 cm^{-1} (imide ring deformation). ^{1}H NMR (DMSO-d_6, δ, ppm): 3.77 (s, -OCH_3), 6.55-7.40 (m, 36H), 7.79 (d, 2H), 7.89 (s, 2H), 7.97 (d, 2H).

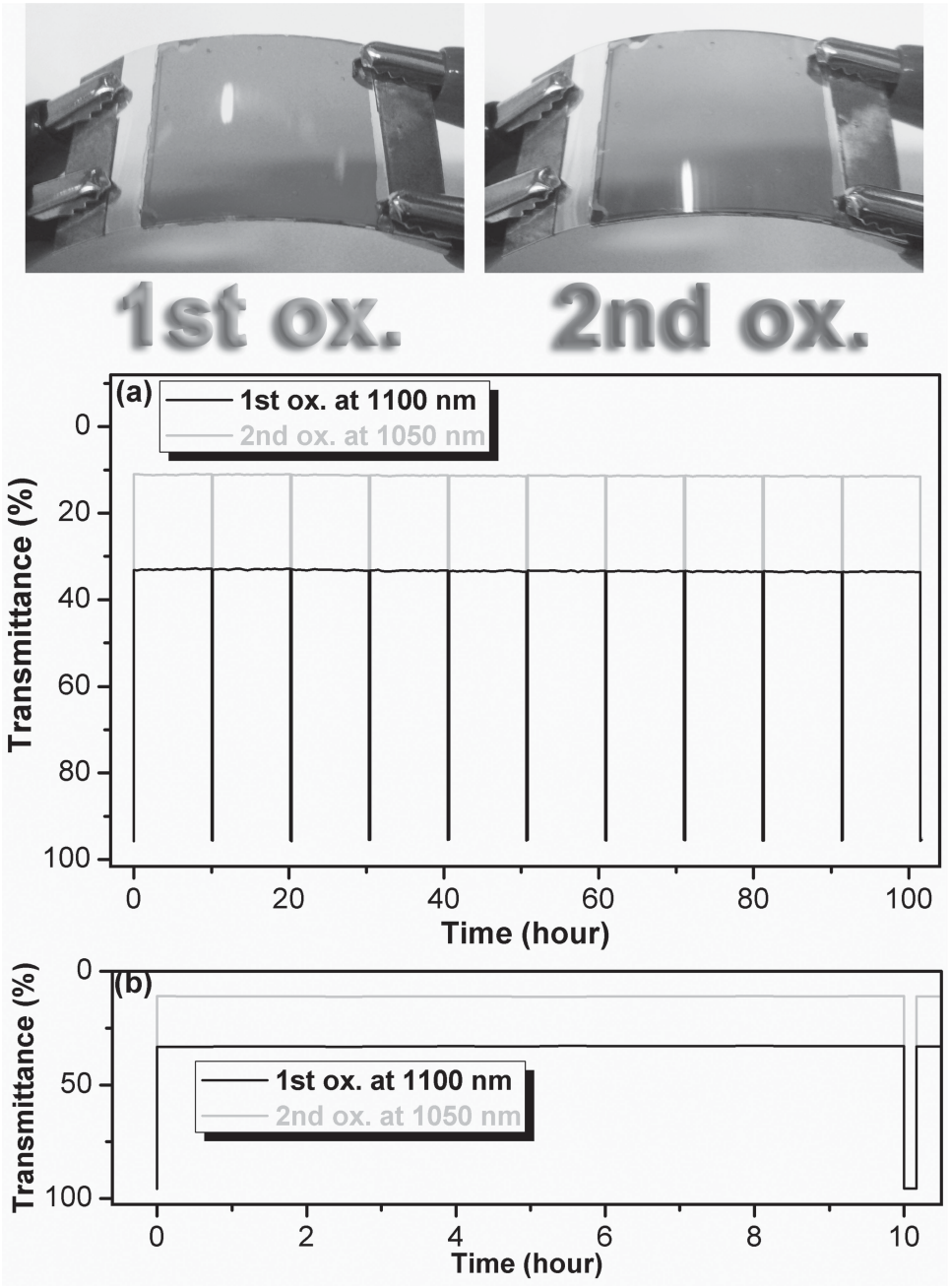

Figure 7. Potential step transmittance change during the continuous cycling test at a) 1st, 2nd oxidized states, and b) transmittance change for 1 switching cycle of a single-layer flexible ITO-coated PEN EC device, using polyimide **9Ph-6FDA** (130 ± 10 nm in thickness) as active layer with a cycle time of 10 h and 10 min for coloring and bleaching processes, respectively.

Preparation of the Polymer Film: A solution of polymer was made by dissolving about 0.2 g of the polyimide sample in 4 mL of DMAc. The homogeneous solution was poured onto a glass substrate (6 cm × 6 cm), which was placed in a 80 °C oven for 5 h to remove most of the solvent, then the semidried film was further dried in vacuo at 160 °C for 8 h. The obtained film was about 20 μm in thickness and was used for solubility test and thermal analyses.

Fabrication of the Flexible Electrochromic Device: Electrochromic polymer film was prepared by coating solution of the polyimide **9Ph-6FDA** (50 mg/mL in DMAc) onto an ITO coated poly(ethylene 2,6-naphthalate) (PEN) (20 mm × 30 mm × 0.3 mm, 20–30 Ω/square) as depicted in Figure 1b. The ITO coated PEN used for memory device was cleaned by ultrasonication with water, acetone, and isopropanol each for 15 min. The polymer was spin-coated onto an active area (20 mm × 20 mm) then dried in vacuum. A gel electrolyte based on poly(methyl methacrylate) (PMMA) (Mw: 350 000) and $LiClO_4$ was plasticized with propylene carbonate (5 g) to form a highly transparent and conductive gel. PMMA (3 g) was dissolved in dry acetonitrile (15 g), and $LiClO_4$ (0.3 g) was added to the polymer solution as supporting electrolyte. The gel electrolyte was spread on the polymer-coated side of the electrode, and the electrodes were sandwiched. Finally, an epoxy resin was used to seal the device.

Fabrication of the Flexible Memory Device: The memory device was fabricated as the configuration of ITO coated PEN/polyimide/Al shown in Figure 1c. A 250 µL DMAc solution of **9Ph-6FDA** (25 mg/ml) was first filtered through 0.45 µm pore size of PTFE membrane syringe filter, then the filtered solution was spin-coated onto the ITO coated PEN at a rotation rate of 1000 rpm for 60 s and heated at 100 °C for 10 min under nitrogen. The film thickness was determined and controlled to be around 50 nm. Finally, a 300-nm-thick Al top electrode was thermally evaporated through the shadow mask (recorded device units of 0.5 × 0.5 mm^2 in size) at a pressure of 10^{-7} torr with a depositing rate of 3-6 Å/s.

Measurements: Fourier transform infrared (FT-IR) spectra were recorded on a PerkinElmer Spectrum 100 Model FT-IR spectrometer. ^{1}H NMR spectra were measured on a Bruker AC-400 MHz spectrometer in DMSO-d_6, using tetramethylsilane as an internal reference, and peak multiplicity was reported as follows: s, singlet; d, doublet. The inherent viscosities were determined at 5.0 g/L concentration using Tamson TV-2000 viscometer at 30 °C. Gel permeation chromatographic (GPC) analysis was carried out on a Waters chromatography unit interfaced with a Waters 2410 refractive index detector. Two Waters 5 µm Styragel HR-2 and HR-4 columns (7.8 mm I. D. × 300 mm) were connected in series with NMP as the eluent at a flow rate of 0.5 mL/min at 40 °C and were calibrated with polystyrene standards. Thermogravimetric analysis (TGA) was conducted with a PerkinElmer Pyris 1 TGA. Experiments were carried out on approximately 6–8 mg film samples heated in flowing nitrogen or air (flow rate = 20 cm^3/min) at a heating rate of 20 °C/min. Thermal mechanical analyzer (TMA) experiment was conducted by a TA instrument TMA Q400 from 40 to 400 °C at a scan rate of 10 °C/min with a film/fiber probe under an applied constant load of 5mN. Electrochemistry was performed with a CH Instruments 611B electrochemical analyzer. Voltammograms are presented with the positive potential pointing to the left and with increasing anodic currents pointing downwards. Cyclic voltammetry (CV) was conducted with the use of a three-electrode cell in which ITO (polymer films area about 0.5 cm × 1.2 cm) was used as a working electrode. A platinum wire was used as an auxiliary electrode. All cell potentials were taken by using a homemade Ag/AgCl, KCl (sat.) reference electrode. Spectroelectrochemical experiments were carried out in a cell built from a 1 cm commercial UV-visible cuvette using Hewlett-Packard 8453 UV-Visible diode array and Hitachi U-4100 UV-vis-NIR spectrophotometer. The ITO-coated glass slide was used as the working electrode, a platinum wire as the counter electrode, and a Ag/AgCl cell as the reference electrode. CE (η) determines the amount of optical density change (δOD) at a specific absorption wavelength induced as a function of the injected/ejected charge (Q) which is determined from the in situ experiments. CE is given by the equation: $\eta = \delta OD/Q = \log[T_b/T_c]/Q$, where η (cm^2/C) is the coloration efficiency at a given wavelength, and T_b and T_c are the bleached and colored transmittance values, respectively. The thickness of the polyimide thin film was measured by alpha-step profilometer (Kosaka Lab., Surfcorder ET3000, Japan). Colorimetric measurements were obtained using JASCO V-650 spectrophotometer and the results are expressed in terms of lightness (L^*) and color coordinates (a^*, b^*). The electrical characterization of the memory device was performed by a Keithley 4200-SCS semiconductor parameter analyzer equipped with a Keithely 4205-PG2 arbitrary waveform pulse generator. ITO was used as common electrode and Al was the electrode for applying voltage during the sweep. The probe tip of a tinned copper shaft with a point radius <0.1 µm was attached to 10 µm diameter tungsten wire (GGB Industries, Inc.). The Gaussian 09 program package is used for theoretical calculation in this research, and the basic units were optimized by means of the density functional theory (DFT) method at the B3LYP level of theory (Beckesstyle three-parameter density functional theory using the Lee-Yang-Parr correlation functional) with the 6-31G(d) basic set.

Supporting Information

Supporting Information is available from the Wiley Online Library or from the author.

Acknowledgements

H.-J.Y. and C.-J.C. contributed equally to this work. We are grateful acknowledge to the National Science Council of Taiwan for the financial support.

Received: February 14, 2013
Revised: March 30, 2013
Published online: May 2, 2013

[1] a) R. H. Friend, R. W. Gymer, A. B. Holmes, J. H. Burroughes, R. N. Marks, C. Taliani, D. D. C. Bradley, D. A. Dos Santos, J. L. Bredas, M. Logdlund, W. R. Salaneck, *Nature* **1999**, *397*, 121; b) Q. Peng, E. T. Kang, K. G. Neoh, D. Xiaob, D. Zou, *J. Mater. Chem.* **2006**, *16*, 376; c) K. Lee, J. Y. Kim, S. H. Park, S. H. Kim, S. Cho, A. J. Heeger, *Adv. Mater.* **2007**, *19*, 2445; d) Y. Shao, G. C. Bazan, A. J. Heeger, *Adv. Mater.* **2008**, *20*, 1191; e) Y. Shao, X. Gong, A. J. Heeger, M. Liu, A. K. Y. Jen, *Adv. Mater.* **2009**, *21*, 1972.

[2] a) G. Yu, J. Gao, J. C. Hummelen, F. Wudl, A. J. Heeger, *Science* **1995**, *270*, 1789; b) C. J. Brabec, N. S. Sariciftci, J. C. Hummelen, *Adv. Funct. Mater.* **2001**, *11*, 15; c) M. H. Chen, J. Hou, Z. Hong, G. Yang, S. Sista, L. M. Chen, Y. Yang, *Adv. Mater.* **2009**, *21*, 4238; d) J. H. Hou, T. L. Chen, S. Q. Zhang, L. J. Huo, S. Sista, Y. Yang, *Macromolecules* **2009**, *42*, 9217; e) A. Kumar, H. H. Liao, Y. Yang, *Org. Electron.* **2009**, *10*, 1615.

[3] a) H. J. Yen, G. S. Liou, *Chem. Mater.* **2009**, *21*, 4062; b) H. J. Yen, H. Y. Lin, G. S. Liou, *Chem. Mater.* **2011**, *23*, 1874; c) H. J. Yen, G. S. Liou, *Polym. Chem.* **2012**, *3*, 255; d) S. V. Vasilyeva, P. M. Beaujuge, S. J. Wang, J. E. Babiarz, V. W. Ballarotto, J. R. Reynolds, *ACS Appl. Mater. Interfaces* **2011**, *3*, 1022; e) E. Puodziukynaite, J. L. Oberst, A. L. Dyer, J. R. Reynolds, *J. Am. Chem. Soc.* **2012**, *134*, 968; f) E. P. Knott, M. R. Craig, D. Y. Liu, J. E. Babiarz, A. L. Dyer, J. R. Reynolds, *J. Mater. Chem.* **2012**, *22*, 4953; g) P. M. Beaujuge, S. V. Vasilyeva, D. Y. Liu, S. Ellinger, T. D. McCarley, J. R. Reynolds, *Chem. Mater.* **2012**, *24*, 255.

[4] a) Q. D. Ling, F. C. Chang, Y. Song, C. X. Zhu, D. J. Liaw, D. S. H. Chan, E. T. Kang, K. G. Neoh, *J. Am. Chem. Soc.* **2006**, *128*, 8732; b) T. J. Lee, C. W. Chang, S. G. Hahm, K. Kim, S. Park, D. M. Kim, J. Kim, W. S. Kwon, G. S. Liou, M. Ree, *Nanotechnology* **2009**, *20*, 135204; c) D. M. Kim, S. Park, T. J. Lee, S. G. Hahm, K. Kim, J. C. Kim, W. Kwon, M. Ree, *Langmuir* **2009**, *25*, 11713; d) K. Kim, S. Park, S. G. Hahm, T. J. Lee, D. M. Kim, J. C. Kim, W. Kwon, Y. G. Ko, M. Ree, *J. Phys. Chem. B* **2009**, *113*, 9143; e) C. L. Liu, W. C. Chen, *Polym. Chem.* **2011**, *2*, 2169; f) C. J. Chen, H. J. Yen, W. C. Chen, G. S. Liou, *J. Polym. Sci. Part A: Polym. Chem.* **2011**, *49*, 3709; g) Y. Q. Li, Y. Y. Chu, R. C. Fang, S. J. Ding, Y. L. Wang, Y. Z. Shen, A. M. Zheng, *Polymer* **2012**, *53*, 229; h) B. L. Hu, F. Zhuge, X. J. Zhu, S. S. Peng, X. X. Chen, L. Pan, Q. Yan, R. W. Li, *J. Mater. Chem.* **2012**, *22*, 520; i) Y. G. Ko, W. Kwon, H. J. Yen, C. W. Chang, D. M. Kim, K. Kim, S. G. Hahm, T. J. Lee, G. S. Liou, M. Ree, *Macromolecules* **2012**, *45*, 3749; j) K. Kim, H. J. Yen, Y. G. Ko, C. W. Chang, W. Kwon, G. S. Liou, M. Ree, *Polymer* **2012**, *53*, 4135; k) Y. C. Hu, C. J. Chen, H. J. Yen, K. Y. Lin, J. M. Yeh, W. C. Chen, G. S. Liou, *J. Mater. Chem.* **2012**, *22*, 20394; l) T. J. Lee, Y. G. Ko, H. J. Yen, K. Kim, D. M. Kim, W. Kwon, S. G. Hahm, G. S. Liou, M. Ree, *Polym. Chem.* **2012**, *3*, 1276; m) T. Kurosawa, T. Higashihara, M. Ueda, *Polym. Chem.* **2013**, *4*, 16.

[5] A. Stikeman, *Technol. Rev.* **2002**, 31.

[6] Y. Chen, B. Zhang, G. Liu, X. Zhuang, E. T. Kang, *Chem. Soc. Rev.* **2012**, *41*, 4688.

[7] A. D. McNaught, A. Wilkinson, *IUPAC Compendium of Chemical Terminology*, 2nd ed., Blackwell Science, Oxford, UK, **1997**.

[8] C. J. Chen, H. J. Yen, W. C. Chen, G. S. Liou, *J. Mater. Chem.* **2012**, *22*, 14085.

[9] a) D. Ma, M. Aguiar, J. A. Freire, I. A. Hummelgen, *Adv. Mater.* **2000**, *12*, 1063; b) S. L. Lim, Q. Ling, E. Y. H. Teo, C. X. Zhu, D. S. H. Chan, E. T. Kang, K. G. Neoh, *Chem. Mater.* **2007**, *19*, 5148; c) H. S. Majumdar, A. Bandyopadhyay, A. Bolognesi, A. J. Pal, *J. Appl. Phys.* **2002**, *91*, 2433; d) E. Y. H. Teo, Q. D. Ling, Y. Song, Y. P. Tan, W. Wang, E. T. Kang, D. S. H. Chan, C. Zhu, *Org. Electron.* **2006**, *7*, 173.

[10] a) S. H. Cheng, S. H. Hsiao, T. X. Su, G. S. Liou, *Macromolecules* **2005**, *38*, 307; b) G. S. Liou, S. H. Hsiao, T. X. Su, *J. Mater. Chem.* **2005**, *15*, 1812; c) G. S. Liou, Y. L. Yang, Y. L. Oliver Su, *J. Polym. Sci. Part A: Polym. Chem.* **2006**, *44*, 2587; d) G. S. Liou, S. H. Hsiao, H. W. Chen, *J. Mater. Chem.* **2006**, *16*, 1831; e) G. S. Liou, S. H. Hsiao, N. K. Huang, Y. L. Yang, *Macromolecules* **2006**, *39*, 5337; f) G. S. Liou, H. W. Chen, H. J. Yen, *J. Polym. Sci. Part A: Polym. Chem.* **2006**, *44*, 4108; g) G. S. Liou, H. W. Chen, H. J. Yen, *Macromol. Chem. Phys.* **2006**, *207*, 1589; h) G. S. Liou, C. W. Chang, H. M. Huang, S. H. Hsiao, *J. Polym. Sci. Part A: Polym. Chem.* **2007**, *45*, 2004; i) G. S. Liou, S. H. Hsiao, W. C. Chen, H. J. Yen, *Macromolecules* **2006**, *39*, 6036; j) G. S. Liou, H. J. Yen, *J. Polym. Sci. Part A: Polym. Chem.* **2006**, *44*, 6094; k) H. J. Yen, G. S. Liou, *J. Polym. Sci. Part A: Polym. Chem.* **2009**, *47*, 1584; l) H. J. Yen, G. S. Liou, *J. Mater. Chem.* **2010**, *20*, 9886; m) G. S. Liou, H. J. Yen, in *Polymer Science: A Comprehensive Reference* (Eds: K. Matyjaszewski, M. Möller), Vol *5*, Elsevier BV, Amsterdam **2012**, pp. 497.

[11] a) C. W. Chang, G. S. Liou, S. H. Hsiao, *J. Mater. Chem.* **2007**, *17*, 1007; b) G. S. Liou, C. W. Chang, *Macromolecules* **2008**, *41*, 1667; c) S. H. Hsiao, G. S. Liou, Y. C. Kung, H. J. Yen, *Macromolecules* **2008**, *41*, 2800; d) C. W. Chang, C. H. Chung, G. S. Liou, *Macromolecules* **2008**, *41*, 8441; e) C. W. Chang, G. S. Liou, *J. Mater. Chem.* **2008**, *18*, 5638; f) C. W. Chang, H. J. Yen, K. Y. Huang, J. M. Yeh, G. S. Liou, *J. Polym. Sci. Part A: Polym. Chem.* **2008**, *46*, 7937; g) H. J. Yen, G. S. Liou, *Org. Electron.* **2010**, *11*, 299; h) L. T. Huang, H. J. Yen, C. W. Chang, G. S. Liou, *J. Polym. Sci. Part A: Polym. Chem.* **2010**, *48*, 4747.

[12] G. S. Liou, H. Y. Lin, *Macromolecules* **2009**, *42*, 125.

[13] M. Robin, P. Day, *Adv. Inorg. Radiochem.* **1967**, *10*, 247.

[14] a) G. Sonmez, H. Meng, Q. Zhang, F. Wudl, *Adv. Funct. Mater.* **2003**, *13*, 726; b) G. Sonmez, H. Meng, F. Wudl, *Chem. Mater.* **2004**, *16*, 574; c) A. L. Dyer, C. R. G. Grenier, J. R. Reynolds, *Adv. Funct. Mater.* **2007**, *17*, 1480; d) M. Li, A. Patra, Y. Sheynin, M. Bendikov, *Adv. Mater.* **2009**, *21*, 1707; e) P. J. Shi, C. M. Amb, E. P. Knott, E. J. Thompson, D. Y. Liu, J. G. Mei, A. L. Dyer, J. R. Reynolds, *Adv. Mater.* **2010**, *22*, 4949; f) P. M. Beaujuge, J. R. Reynolds, *Chem. Rev.* **2010**, *110*, 268; g) C. M. Amb, A. L. Dyer, J. R. Reynolds, *Chem. Mater.* **2011**, *23*, 397.